

Figure 2 | Faraday rotation in the bursts. **a**, **b**, Variations of the Stokes parameters Q (**a**) and U (**b**) with frequency, normalized by the total linear polarization ($L = \sqrt{Q^2 + U^2}$), for the six brightest Arecibo bursts detected on modified Julian date 57,747. Different bursts are plotted using different colours. Only data points with signal-to-noise ratio higher than 5 are

plotted and do not include uncertainties. The black lines represent the best-fitting Faraday rotation model for the global values reported in Table 1. **c**, Difference between calculated and measured polarization angles (ΔPA) with 1σ uncertainties around the central values, which are indicated with black dots.

rotation measure (below about 50 rad m^{-2}) and polarization angle (lower than approximately 10°) between bursts. The GBT data are not well modelled by the use of a single $PA_{\infty}^{\text{global}}$ value, but this could be an instrumental difference or reflection of the higher observing frequency. The near constancy of the polarization angle suggests that the burst emitter has a stable geometric orientation with respect to the observer. A linear polarization fraction higher than about 98% at a single rotation measure constrains turbulent scatter¹⁹ as $\sigma_{\text{RM}} < 25 \text{ rad m}^{-2}$ and the linear gradient across the source as $\Delta_{\text{RM}} < 20 \text{ rad m}^{-2}$, and there is no evidence of deviations from the squared-wavelength (λ^2) scaling of the Faraday rotation effect. Analysis with the RM Synthesis technique and the deconvolution procedure RMCLEAN also implies a ‘Faraday-thin’ medium (see Methods).

In the rest frame, the host galaxy contributes a dispersion measure $DM_{\text{host}} \approx 70\text{--}270 \text{ pc cm}^{-3}$ to the total dispersion measure of the bursts⁸. Given RM_{src} , this corresponds to an estimated line-of-sight magnetic field $B_{\parallel} = 0.6f_{\text{DM}} - 2.4f_{\text{DM}} \text{ mG}$. This is a lower-limit range because the dispersion measure contribution that is related to the observed rotation measure (DM_{RM}) could be much smaller than the total dispersion measure contribution of the host (DM_{host} , dominated by the star-forming region), which we quantify by the scaling factor $f_{\text{DM}} = DM_{\text{host}}/DM_{\text{RM}} \geq 1$. For comparison, typical magnetic field strengths within the interstellar medium of our Galaxy²⁰ are only about $5 \mu\text{G}$.

We can constrain the electron density, electron temperature (T_e) and length scale (L_{RM}) of the region causing the Faraday rotation by balancing the magnetic field and thermal energy densities (Extended Data Fig. 6). For example, assuming equipartition and $T_e = 10^6 \text{ K}$, we find a density of $n_e \approx 10^2 \text{ cm}^{-3}$ on a length scale of $L_{\text{RM}} \approx 1 \text{ pc}$, comparable to the upper limit of the size of the persistent source¹⁰.

A star-forming region, such as that hosting FRB 121102, will contain H II regions of ionized hydrogen. Although very compact H II regions have sufficiently high magnetic fields and electron densities to explain the large rotation measure, the constraints from DM_{host} and the absence of free-free absorption of the bursts exclude a wide range of H II region sizes and densities²¹ for typical temperatures of 10^4 K .

The environment around a massive black hole is consistent with the n_e , L_{RM} and T_e constraints²², and the properties of the persistent source are compatible with those of a low-luminosity, accreting massive black hole¹⁰. The high rotation measure towards the Galactic Centre magnetar²³ PSR J1745–2900 (Fig. 3), $RM = -7 \times 10^4 \text{ rad m}^{-2}$, provides an intriguing observational analogy for a scenario in which the bursts are produced by a neutron star in the immediate environment of a massive black hole. However, the bursts of FRB 121102 are many orders of magnitude more energetic than those of PSR J1745–2900 or any Galactic pulsar.

An alternative description of FRB 121102 has been proposed by a millisecond magnetar model^{8,10,13}. According to that model, one would expect a surrounding supernova remnant and nebula powered by the central neutron star. The n_e , L_{RM} and T_e constraints are broadly compatible with the conditions in pulsar-wind nebulae, but dense filaments like those seen in the Crab Nebula²⁴ may need to be invoked to explain the high and variable rotation measure of FRB 121102. In a young neutron star scenario, an expanding supernova remnant could also in principle produce a high rotation measure by sweeping up surrounding ambient medium and progenitor ejecta²⁵. A more detailed discussion of these scenarios is provided in Methods, and more exotic models also remain possible²⁶.

Regardless of its nature, FRB 121102 clearly inhabits an extreme magneto-ionic environment. In contrast, Galactic pulsars with comparable dispersion measures have rotation measures that are

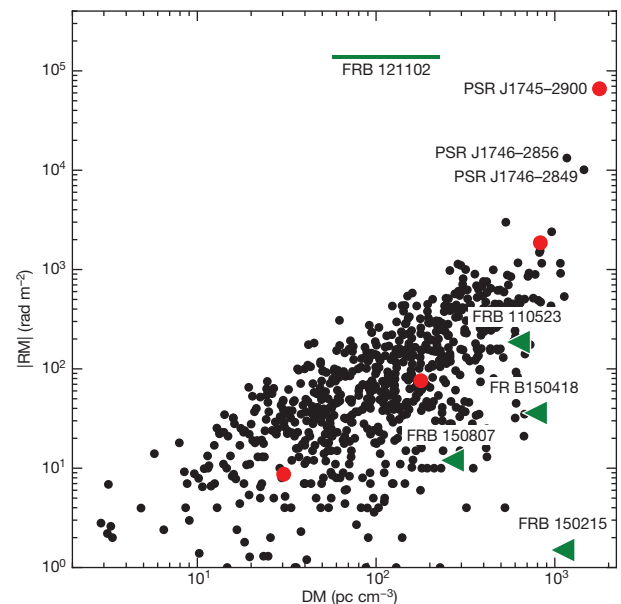


Figure 3 | Magnitude of rotation measure versus dispersion measure for fast radio bursts and Galactic pulsars. Radio-loud magnetars are highlighted with red dots, while radio pulsars and magnetars closest to the Galactic Centre³⁰ are labelled by name. The green bar represents FRB 121102 and the uncertainty on the dispersion measure contribution of the host galaxy⁸. Green triangles are other fast radio bursts with measured rotation measure; here the dispersion measure is the upper limit of the contribution from the host galaxy.